VERSITA

Acta Geophysica
vol. 57, no. 1, pp. 220-235
DOI: 10.2478/s11600-008-0079-x

The Planeterrella, a Pedagogic Experiment in Planetology and Plasma Physics

Jean LILENSTEN[1], Mathieu BARTHÉLEMY[1], Cyril SIMON[2], Philippe JEANJACQUOT[3], and Guillaume GRONOFF[1]

[1]Laboratoire de Planétologie de Grenoble, OSUG-CNRS-UJF, Grenoble, France
e-mails: jean.lilensten@obs.ujf-grenoble.fr (corresponding author),
mathieu.barthelemy@obs.ujf-grenoble.fr, guillaume.gronoff@obs.ujf-grenoble.fr

[2]Belgian Institute for Space Aeronomy and B.USOC, Brussels, Belgium
e-mail: cyril.simon@gmail.com

[3]Lycée Charlie Chaplin, Décines, France; e-mail: philippe.jeanjacquot@gmail.com

Abstract

We present here a plasma physics experiment which makes it possible to simulate, in a naive yet useful way, the formation of polar lights. It involves shooting electrons at a magnetized sphere placed in a vacuum chamber. This experiment, inspired by K. Birkeland's *Terrella*, built at the turn of 19th century, allows the visualization of very many geophysical and astrophysical situations. Although delicate, it is feasible at undergraduate level.

Key words: Aurora, planetary ionospheres, plasma, the Planeterrella experiment.

1. THE TERRELLA: KRISTIAN BIRKELAND'S HISTORICAL EXPERIMENT

In 1733, in the first treatise on the aurora borealis (or polar lights), Jean-Jacques Dortous de Mairan describes in an intuitive but visionary way the bond between the aurorae and the Sun: "It is certain, as we shall demonstrate from a great number of observations which are not ambiguous, that the Atmosphere of the Sun […] reaches sometimes the Terrestrial Orbit. At that time the matter which composes this Atmosphere suddenly meets the higher parts of our air, below the limits where universal Gravity, whatever the cause, starts to act with more force towards the center of the Earth than towards the Sun, falls into the Earth's atmosphere to more or less depth, according to whether specific gravity is more or less large, with regards to the layers of air which it crosses, or which it survives." A few years later, in 1747, the Swedish astronomer Anders Celsius and his assistant Olof Hiorter discover that the magnetic field is an essential ingredient of the physics of the aurorae borealis. During the 19th century, geographers establish that the polar lights occur preferentially around the magnetic poles, drawing what will be called the "auroral ovals". Parallel works in electromagnetism also result in postulating the existence of charged particles, the electrons, soon discovered by Thomson in 1901. These charged particles were at that time given the name "cathode rays".

At the end of the 19th century, the Norwegian physicist Kristian Birkeland, a brilliant experimenter, had the original idea to shoot cathode rays on a magnetized sphere suspended in a vacuum chamber. He imagined the cathode to represent the Sun with the cathode rays simulating the solar atmosphere for which Parker will coin the term "solar wind" in 1958, and the suspended magnetized sphere representing the Earth. He built up to fourteen different versions of his experiment during the course of his life. This experiment is called *Terrella*. It made it possible to make the first laboratory demonstration of the mechanism of the polar lights by reconstructing and visualizing the auroral ovals. The notes of Birkeland are not very precise, but his experiment was recently rebuilt at the University of Tromsø (Norway) by the engineer Terje Bruntdland starting from the original experiment. This allowed determining the necessary vacuum conditions to be about a few pascals, while the electric tension was of a few hundred volts.

By reversing the polarities of his experiment, Birkeland was also the first to visualize the ring currents. The radiation belts associated to these currents were later discovered in 1958 during the first US space flights by James Van Allen, a result which earned him the Crafoord prize in 1989. Unfortunately, Birkeland gave a bad interpretation to his observation, comparing the rings he saw to Saturn's rings.

With the advent of the space age (Egeland and Burke 2005), it was understood that the aurorae are produced primarily by electrons accelerated via electric potentials resulting from plasma convection flows in the Earth's magnetosphere. These flows are ultimately caused by the solar wind plasma flowing past the Earth, which couples energy and momentum across the Earth's magnetosphere boundary via magnetic reconnection (Stern 1996, Kivelson and Russel 1995, Lilensten and Bornarel 2006). None of these essential physical processes were incorporated into Birkeland's original experimental design and neither are they in the newly designed experiment. However, we will show that there is still interest in building a *Terrella* or, better, a *Planeterrella*.

2. A NEW EXPERIMENT: THE PLANETERRELLA

We designed a new experiment which allows many other possibilities. Instead of Birkeland's hanging globe, which made his experimental setup very difficult to modify, the hollow sphere is put on a base which one can freely move and adjust in height. The magnetic axis of the rare earth magnet can be pointed in any desired direction inside the sphere. The electrode is attached to a wheel inserted into a notch, embedded in a bent plastic structure. Thus, it can be moved and positioned in all directions around its axis (Fig. 1). Contrary to the original *Terrella*, one can multiply the number of spheres and thus look at interactions in multiple configurations. We use a vacuum chamber 50 liters (5×10^{-2} m^3) in volume and 50 cm in diameter. The two aluminium spheres (Birkeland used copper) have diameters, respectively, of 10 cm and 5 cm. The vacuum is about 10 Pa. The tension is higher than 300 V for

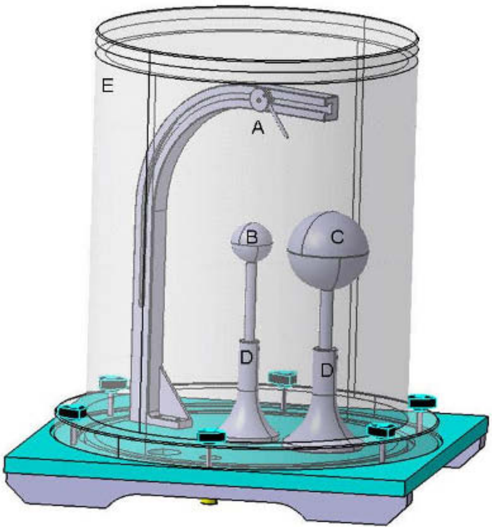

Fig. 1. Experimental design of *the Planeterrella*. A is the electrode attached to a wheel free to run along a channel inserted in a curved plastic structure; B is the 5-cm diameter hollow sphere; C is the 10-cm diameter hollow sphere. The rare earth magnets are positioned in the sphere with a variable magnetic axis; D is the adjustable bases; E is the vacuum chamber (50 l). The electric configuration is flexible: the electrode and the spheres (or only one sphere) can be plugged freely to the anode or cathode of the power supply. Colour version of this figure is available in electronic edition only.

an intensity on the order of 0.1 to 1.0 mA. For simplicity in the numerical applications, we will take a value of 1000 V and 0.1 mA. The emitted electrons then have a maximal potential energy of 1 keV or 1.609×10^{-16} J. The intensity of the magnetic field is approximately 0.5 T at 0.5 cm of the surface of the magnets, which have a size of a half centimeter.

Observations

All the configurations observed by Birkeland are reproducible. In Fig. 2, one sees the two auroral ovals. Here, the sphere is the anode and the duct is the cathode. When the sphere becomes the cathode, a radiation belt appears (Fig. 3), but there are many additional possibilities.

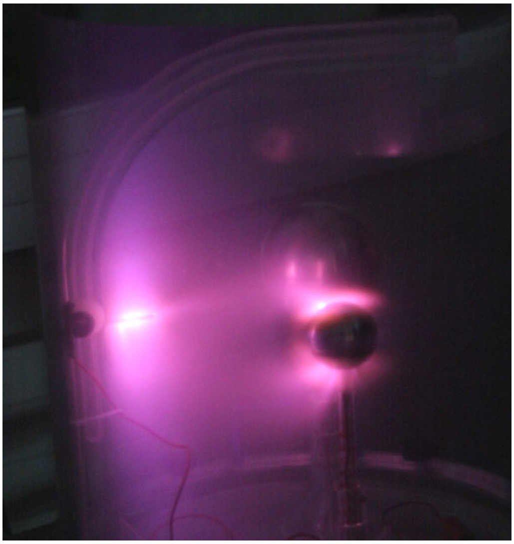

Fig. 2. *The Planeterrella* in Birkeland's configuration. The cathode is positioned at the left of the picture. It is glowing as well. The hollow sphere is the anode. The magnetic axis inside the sphere is perpendicular to the electron beam. Two ovals appear on each hemisphere (credit: J. Aboudarham, LESIA-OPM). Colour version of this figure is available in electronic edition only.

A better visualization of the phenomena

Rather than using the electrode duct as an electron gun, one can now use one sphere as the cathode (the star) and another as the anode (the planet). This is shown in Fig. 4. In the foreground, the star-cathode is magnetized. One sees the coronal halo with the coronal hole above the pole, comparable with those observed on the Sun. In the background, the auroral ovals are formed on a magnetized planet but the Van Allen belt is now visible. It is however

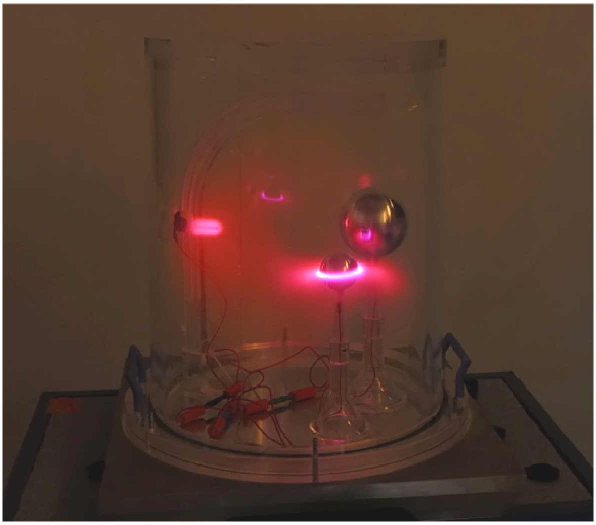

Fig. 3. The electrode is in the anode configuration at the left of the picture, while the small sphere is the cathode. The large sphere is not connected to the electric circuit and is here only to show the experimental design. The ring in the middle is a reflection of the small sphere on the vacuum chamber (credit: C. Simon, LPG/BISA). Colour version of this figure is available in electronic edition only.

Fig. 4. Interaction between a magnetized star (the large sphere) and a planet (the small one). On the large sphere (the cathode), the electrons are emitted around the magnetic poles which are tilted *versus* the vertical axis. A "coronal hole" may be seen exactly where the magnetic pole stands. On the small sphere (the anode), a ring current surrounds the "planet" closing on the auroral ovals, similar to the Van Allen belt (credit: G. Gronoff, LPG). Colour version of this figure is available in electronic edition only.

necessary to take care not to push the analogy too far: the coronal holes are of course related to the solar magnetic field, but also to the dynamics of the star.

Planets with tilted magnetic axes

In Table 1, we list the values of the magnetic field parameters of various planets. Saturn is a curiosity, since its magnetic and geographic poles are aligned. The Earth and Jupiter have magnetic declinations of about 10°. It is

Table 1

Magnetic field parameters for various planets

Planets	Rotation [hour]	Magnetic momentum	Magnetic field at equator [10^{-4} T]	Magnetic angle with respect to geographic axis
Mercury	1404	4×10^{-4}	2×10^{-3}	?
Earth	24	1	0.31	11.3°
Jupiter	9.9	20	4.28	–9.6°
Saturn	10.7	600	0.22	0°
Uranus	7.2	50	0.23	–59°
Neptun	16.1	25	0.14	–47°

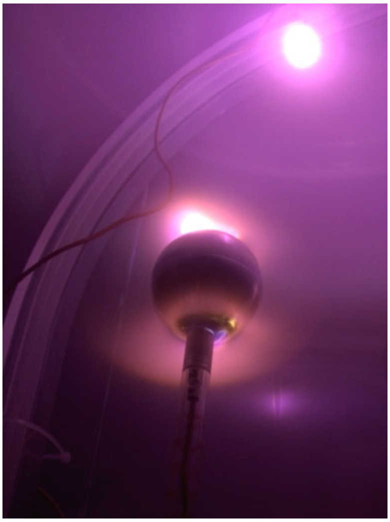

Fig. 5. The cathode (the electric duct at the top of the screen) faces a magnetic pole of the small sphere, representing Uranus. On the “dayside” of this planet-like, an auroral spot develops at the place of the magnetic pole. On the “nightside”, one sees an auroral oval (credit: G. Gronoff, LPG). Colour version of this figure is available in electronic edition only.

this configuration that Birkeland always privileged. The simple fact of being able to position the spheres as needed and to allow the electrode to move makes it very easy the incline the magnetic field inside the sphere. One can thus simulate the configurations of Neptune and Uranus, whose magnetic angles are about 50°. The geographical North Pole of Uranus points towards the Sun, so that its magnetic axis is almost directed like that of the Earth with respect to the solar wind. The Voyager probe has already detected a dayside aurora on Uranus, close to its magnetic pole. The angle of inclination of the axis of rotation of Neptune on the ecliptic is 29°, with an angle of 45° between the magnetic and geographical axes. Thus the solar wind enters directly into the polar cap. This is visible in Fig. 5. But much more can be seen in this figure. Indeed, on the “night” side of the sphere, a large auroral oval shows up. If this simulation can be considered as a good analogy (see Section 4), ***Uranus should therefore have a nightside auroral oval***. That is what future space missions will confirm or infirm.

Other vizualisations

The experiment allows to visualize several other interactions, not illustrated here.

On December 12, 1996, “Nature” published the discovery of Dr. Kivelson and his colleagues of the magnetic field of Ganymede, satellite of Jupiter (Kivelson *et al.* 1996). The magnetic fields of Io and Europa were discovered shortly after. The configuration with several spheres makes it possible to simulate the auroral interactions of these bodies. Such interactions between a magnetized planet and a magnetized satellite may be simulated with the experiment. It goes without saying that scaling problems can arise, and that it is therefore necessary to be very careful with the interpretation of the observations. But numerous configurations representing the interaction between a magnetized exoplanet and a near magnetized star can then be imagined. Indeed, more than a hundred exoplanets have been discovered since 1995 (http://exoplanet.eu/catalog.php). Because of the methods of detection, most are “Jupiter-like” planets in term of size, with very short distances from their star (for example 0.04 Astronomical Units for HD179949b). Nothing excludes that these planets, like their star, can be magnetized. In this case, the short distance between them implies direct magnetic interactions, their fields recombining without the generation of a magnetosphere. This case can also be shown in the current configuration of the experiment.

Another example is to look at binary systems. Since each sphere and the electrode are connected to an electric plug, we can also easily simulate the electromagnetic interaction of two-star systems (binary stars) with planets in all magnetic configurations.

The Planeterrella

The configurations of the experiment suggested here are very numerous. It is now possible to simulate the majority of the cases encountered in planetology. This is why we named this experiment *Planeterrella*.

3. PHYSICS OF THE PHENOMENON

We wish to give a first approach of the physics of this experiment. Many things can be studied such as Maxwell's equations, plasma physics, radiation and the quantum states of the molecules. We will rather focus here on some plasma physics properties, without considering the effect of the thermal collisions.

We consider the historical setup of Birkeland, where an electrode duct is used as the cathode and the anode is the magnetized sphere. The x axis is aligned along the duct-center of the sphere axis. The magnetic North-South axis is perpendicular to x, defining the axis z. The distance between the cathode and the center of the sphere is 30 cm. Many text books demonstrate the equations given below (the authors like in particular Chen 1984, Balescu 1988, Shu 1992, and Dendy 1995).

Characteristics of the neutral gas

By using the ideal gas law for a constant temperature T of 300 K, we can easily deduce the density inside the chamber:

$$\frac{N}{V} = \frac{P}{k_B T} ,$$

where N is the particle number, V is the volume, P is the pressure, T is the temperature, and k_B is the Boltzmann constant.

The neutral density n_n we can derive is of the order 2×10^{21} m^{-3}. It is interesting to note that this corresponds to the concentration of the terrestrial atmospheric gas around 70 km, i.e., relatively close to the altitude region where aurorae occur (typically between 80 and 300 km). Birkeland was lucky that the vacuum he could perform in his chamber was precisely that one: more or less pressure would not have allowed the same observations, while the existence of an upper atmosphere was not even conceived at that time.

Suprathermal electron characteristics

The electrons shot by the cathode have a high energy; as an analogy with the physics of space environments, we call them "suprathermal electrons". From the kinetic energy equation, their maximal velocity is 1.88×10^7 m s^{-1}, i.e., 6% of the speed of the light, which makes them non-relativistic. Because the electric field constraints the suprathermal electrons in one direction, the suprathermal electron temperature is deduced from $E = k_B T_e^s$. Its value is 1.17×10^7 K. This temperature is the maximum reachable and is only valid for electrons which do not collide during their travel in the medium.

The electrons resulting from the impact ionization between the suprathermal electrons and the neutral gas do not have a Maxwellian distribution. We call them the ambient electron population. They experience collisions that rapidly thermalize them. However, they are ejected with a large energy. Following Dendy (1995), we will consider a mean energy of 1 eV, i.e., a mean temperature T_e of 1.1×10^4 K.

Ambient electron density

Collisions between the suprathermal electrons and the neutral gas in the vacuum chamber create, amongst other phenomena, ionization. We now compute the ambient electron density in the part of the chamber where the suprathermal electrons propagate, making a cone going away from the electrode and towards the sphere placed at 30 cm. The volume of this cone is about 500 cm^3. The ionization in this cone occurs all along the electron trajectory mainly because the energy of the electrons is much higher than the ionization cross section threshold. In the Earth's ionosphere, comparative phenomena have been described (Rees 1989) and the ionization along the electron trajectory in a gas chamber was studied (Lummerzheim and Lilensten 1994). The atmospheric gas consists of two species of diatomic homonuclear molecules, N_2 and O_2. We assume that they behave like an equivalent molecule M_2. Consequently, the ambient electrons undergo only one reaction, a recombination $e^- + M_2^+ \rightarrow M_2$. As M_2 is a virtual molecule, the kinetics is described through an efficiency coefficient α_{eff}. In the atmosphere, α_{eff} varies with altitude. At around 70 km, its value is approximately 10^{-9} cm^3 s^{-1}. The stationary continuity equation for electrons is reduced due to the fact that productions and losses balance each other. Losses are computed from the chemical equation of recombination: $Losses = \alpha_{eff} N_e [M_2^+]$, where N_e represents the ambient electron density. The ambient plasma is considered globally neutral: there are as many ions as there are electrons. This assumption is called the plasma approximation. Then $Losses = \alpha_{eff} N_e^2$.

The chemical equilibrium equation enables us to write

$$N_e = \sqrt{\frac{\text{production}}{\alpha_{eff}}} \;.$$

We compute the production considering that a suprathermal electron expelled by the cathode gives away 35 eV on average to create an electron-ion pair $\{e^-, M_2^+\}$ [11]. Thus, each initial electron produces 1000/35 $\{e^-, M_2^+\}$ pairs. With an intensity of 10^{-4} A, we obtain a flux of $10^{-4}/1.609\times10^{-19}$ = 6.215×10^{14} electrons ejected by the cathode per second. The production of $\{e^-, M_2^+\}$ pairs per second is then

$$\frac{10^{-4}}{1.609\times10^{-19}}\frac{1000}{35} = 1.78\times10^{16}\ \mathrm{s}^{-1}.$$

In the useful volume of 0.5 liter, we obtain a production rate of 3.56×10^{13} cm^{-3} s^{-1}. We can now place this value in the electron density equation to find $N_e = 2\times10^{17}$ m^{-3}.

It is interesting to compare this value to that of the suprathermal electron density. An intensity of 0.1 mA corresponds to a flux of 6.215×10^{14} electrons per second. Dividing by the velocity one gets the number of electrons per meter along the path. Although the electrons are distributed in a cone, let us consider that their path is 0.3 m long for all of them (which will give an upper limit for the suprathermal electron density). Multiplying by this length gives the total number of electrons. Finally, we consider that these electrons are confined to the 0.5-liter volume. The suprathermal electrons density is then

$$N_e^s = \frac{10^{-4}}{1.609\times10^{-19}}\frac{1}{1.88\times10^{7}}\frac{0.3}{5\times10^{-4}} = 2\times10^{10}\mathrm{cm}^{-3}\ .$$

This is 10,000 times smaller than the ambient electron density: the plasma approximation is therefore valid, although considering that the speed is clearly overestimated.

Close to the electron gun: the Debye screening and the cathode fall

We will now consider that, close to the electrode, the effect of the magnetic field is negligible in front of that of the electric field (we will check this assumption later). The ions created (primarily N_2^+ and O_2^+) by collisions with the suprathermal electrons in the vacuum chamber will gather close to the cathode and create an electric screen. This well-known phenomenon is called the Debye screen. It is at work in the Earth's upper atmosphere, and is at the basis of the incoherent scatter radar theory. In order to write the equation, one must consider that the screening is at work for an ion density exactly equal to the suprathermal electron density, while the ion temperature is the ambient temperature $T = 300$ K. Poisson's equation is written as $\nabla\mathbf{E}=\rho/\varepsilon_0$.

Since the electric field derives from a potential, $\mathbf{E}=-\nabla V$, one gets

$$\frac{\mathrm{d}^2V}{\mathrm{d}x^2}=\frac{\rho}{\varepsilon_0}\ .$$

The Maxwell-Boltzmann statistics yields at the first order: $\rho=e\,N_e^s\,\frac{eV}{k_bT}$, where e represents the electric charge. While inserting this value of the charge density in the second derivative, we can integrate the potential

$$V=V_0\exp\left(-\frac{|x|}{\lambda_D}\right),$$

where λ_D is called the Debye length; it represents the characteristic size beyond which the field is completely screened by the positive charges

$$\lambda_D=\sqrt{\frac{\varepsilon_0\,k_B\,T}{N_e^s e^2}}\ .$$

A region of several Debye lengths is created where the electric potential drops and the electric field is strong. The size of this region is $\zeta=\frac{4}{3}\left(\frac{\eta}{2}\right)^{3/4}$ in unit of the Debye length with $\eta=\left|-e\phi/k_BT_e\right|$ and ϕ is the potential drop through ζ. Considering a complete screening with $\phi=1000$ V, we find $\lambda_D=0.016$ mm and $\zeta=140$. The size of the cathode fall region is approximately 2.3 mm. Beyond this distance from the cathode the potential variation is null at first approximation (it is lower than 1 V). There is no more acceleration due to the electric field and the electrons propagate at a constant speed, the initial direction of which is parallel to the direction of the electric field that accelerated them. The cathode fall region corresponds to a dark region very close to the cathode, easily seen in *the Planeterrella* experiment.

Is it correct to neglect the magnetic field effect close to the electrode? Inside the Debye sphere, the electric field can be estimated using $\mathbf{E}=-\nabla V$. By taking 1000 V and a distance of 1 cm, $|E|=10^5$ V·m^{-1} in a first approximation. The magnetic field is dipolar and decreases according to the cube of the distance: $B/r^3=$ const. Measuring a magnetic field of 0.5 T at a distance of 0.5 cm, we calculate a value of 2.3×10^{-6} T close to the electrode at 30 cm. The $\boldsymbol{v}\times\boldsymbol{B}$ term of the Lorentz force equals 4.3×10 V·m^{-1}, which is negligible in comparison to $|E|\sim10^5$ V·m^{-1}.

The generation of the ring current

Beyond the Debye sphere, the electric field is not taken into account anymore. Let us initially consider a constant magnetic field. The Lorentz force is $\mathbf{F} = q\mathbf{v}\times\mathbf{B}$. While projecting on (x, y, z) axes, the electrons are subject to a rotation with a cyclotron frequency given by

$$\omega_c = \frac{|q|B}{m}$$

and a radius (called Larmor radius) given by

$$r_L = \frac{v_\perp}{|\omega_c|} = \frac{m v_\perp}{|q|B} .$$

To calculate the values of these parameters, it is sufficient to consider the relation of the dipolar field $B/r^3 = \text{const}$ with a value of 0.5 T measured at the edge of the magnet at 0.5 cm. The assumption is also made that the perpendicular velocity is equal to the initial velocity of the suprathermal electrons, that is to say $1.88\times10^7\,\text{m}\,\text{s}^{-1}$ as computed above. The values for some distances are given in Table 2.

Table 2

Cyclotron frequencies and Larmor radiuses
for some distances to the magnet center

	0.5 cm	2.5 cm	5 cm	30 cm
Cyclotron frequency	8.8×10^{10} s^{-1}	7×10^8 s^{-1}	8.8×10^7 s^{-1}	10^5 s^{-1}
Larmor radius	0.21 mm	2.7 cm	21 cm	188 m

Then, the presence of a magnetic field generates a rotation. But a second effect is at work, due to the gradient of the magnetic field. While approaching the magnet, the electrons cross a medium in which the gradient of the field increases. The classical theory is limited to a first-order development. In this case, by neglecting at the moment the effects of the collisions, the equation of forces is written as

$$\mathbf{F} = q\left(-\frac{r_\perp v_\perp}{2}\nabla B + \mathbf{v}\times\mathbf{B}\right) .$$

With the stationarity assumption, this sum equals zero. This implies that the electrons are subject to a drift:

$$\mathbf{v} = -\frac{r_\perp v_\perp}{2}\frac{\mathbf{B}\times\nabla B}{B^2} .$$

The electron drift is both perpendicular to the field and to the gradient of the field, making a rotation around the magnet, origin of the ring current.

Effect of the collisions

The collisions take place all along the trajectory of the suprathermal electrons. They are characterized by a collision frequency ν_{coll} which values (expressed in units per second) are mainly based on experimental measurements of collision cross sections:

$$\nu(e^-, \mathrm{N_2}) = 2.33\times10^{-17}[\mathrm{N_2}]\left(1-(1.21\times10^{-4})T_e\right)T_e \ ,$$

$$\nu(e^-, \mathrm{O_2}) = 1.82\times10^{-16}[\mathrm{O_2}]\left(1+(3.6\times10^{-2})T_e\right)\sqrt{T_e} \ .$$

For numerical application, one shall consider that the Earth's atmosphere is composed of 1/3 of molecular oxygen and 2/3 of molecular nitrogen. The most interesting place with respect to the collisions is in the ring current. Indeed, the electrons turning on a constant radius can be seen as being subject to a constant field. The effect of the collisions is then primarily to give them a vertical impulse, which projects them into a shell whose feet on the sphere, on north and the south, are rings which are projections of the ring of current. As the magnetic field tubes are tightening close to the poles, the number of excitations per unit area increases, and the emitted radiation becomes intense enough to be visible. One could go further and study the effect of magnetic mirroring, which causes the return of the electrons from an hemisphere towards the other, but this effect does not have an influence on the observation.

Emission lines observed in the Planeterrella experiment

The collisions between the suprathermal electrons and the ambient gas create excited molecules and ions that are possibly excited too. Deexcitations can occur following several paths: electronic recombination for the ions, chemical reactions, or radiative emission. These are the emissions which are observed in *the Planeterrella*. They occur all along the trajectory of the suprathermal electrons, but are more intense where their density is higher, either in the ring current, or in the auroral ovals.

We will now discuss the different observed emission lines. We observe the spectral lines of molecular oxygen and molecular nitrogen. Concerning the molecular oxygen, the entire range from 300 to 440 nm is dominated by two systems of bands: Herzberg and Chamberlain. The excitation of molecular oxygen in the state $A^3\Sigma_u^+$ comes from the three-body collision between two oxygen atoms and a third body, molecule or atom. The transition which goes from the $A^3\Sigma_u^+$ state to the ground state violates the rule according to which one cannot go from a Σ^+ state to a Σ^- state. The Schumann-Runge system emits in a quasi-continuum between 125 and 175 nm. The ground state of molecular nitrogen is the state $X^1\Sigma_g^+$ while the ground state of the N_2^+ ion is $X^2\Sigma_g^+$. A special characteristic of the spectrum of the excited molecular nitrogen is the cascade generating the second positive band, the first positive band and the Vegard-Kaplan band, sometimes wrongly referred to as the molecular nitrogen triplet. The $C^3\Pi_u$ state has a short lifespan, about 10^{-7} s. It has only one source, which is the collision of a nitrogen molecule with an energetic electron, and only one sink, the deexcitation towards the state $B^3\Pi_g$. This characteristic makes it an ideal tracer of the deeexcitation rate through electron collision. The second positive band has lines between 320 and 380 nm, but 86% of the $C^3\Pi_u$ population are in the state $\chi = 0$ or 1. In addition, 49% of the $\nu' = 0$ state are deexcited while emitting to 337.1 nm, which is one of the most intense lines visible in *the Planeterrella*. The second positive band radiates in the blue range, also quite visible, and in the ultraviolet. The first positive band results from the deexcitation of the $B^3\Pi_g$ state. In the Earth's atmosphere, this band is very intense but also divided into many excited levels on a broad spectral range. It plays a major role in the analysis of the diurnal radiation, and is used as a tool to measure the total excitation rate by electron collisions. The first positive band emits mainly between 600 and 750 nm, i.e. in the red, and can be identified in the Planeterrella experiment as well.

4. LIMITS AND FUTURE EXTENSIONS OF THE EXPERIMENT

The observations made with the Planeterrella are easy to reproduce, even if the experiment can prove to be delicate to set up. We must also be careful not to draw general conclusions from these observations or to make them tell more than what they actually are. The space environment of magnetized planets is very complex. The cathode in Birkeland's configuration does not represent the Sun as he believed but more the plasma sheet contained in the equatorial plan of the magnetosphere. In our experiment, there is also no acceleration phenomenon: the electrons are produced by a relatively stable generator. When varying this tension, it is impossible to simulate the interactions occurring in the solar wind between slow and fast winds, a phenomenon responsible of the auroral curtains observed from Earth.

Before using this experiment for scientific purposes, several steps have to be taken. First of all, it is necessary to solve a difficult problem of scales and to prove that the configurations reproduce the natural phenomena correctly. It is indeed quite surprising that *the Planeterrella* reproduces so well natural phenomena that occur at such different scales: volumes of the space bodies, natural electric and magnetic fields and distances are absolutely not respected in the experiment. It is also necessary to carry out a rigorous calibration. Despite this, this experiment can already be extended easily.

The first important evolution will be to use electromagnets of variable magnetic intensity. At the moment, we use an artifact while placing magnets close to the internal surface of the spheres. This results in the creation of separated dipoles, breaking the ideal dipolar configuration (all configurations shown in this paper are made with a single magnet placed in the center of the spheres in order to maintain a dipolar field). A second evolution consists in putting the spheres in motion, in particular to authorize their rotation. Please observe, however, that the auroral oval is not related to the rotation of a planet through gravity, but through the precession of the magnetic axis around the geographical axis. Allowing the spheres to turn would show in a very spectacular way how the ovals move with the tilt of the field.

Following these modifications, and for the study of the dynamics, the evolution currently studied is the installation of two cameras placed in two different orientations in order to obtain a stereoscopic and dynamic image of the Planeterrella. The coupling with spectrometers will in the long term allow the spectral study of the emission lines.

To tackle scientific simulations, we envisaged a passage for the injection of gases in order to reproduce the recently discovered Martian aurorae (Bertaux *et al.* 2005), and the action of the solar wind in the upper atmosphere of Venus.

5. CONCLUSIONS

This experiment has already been performed at a high school level with materials from the school. The great difficulty comes from the manufacture of the spheres. Those must have a good surface quality, because any irregularity can divert the electric field. We used the end balls of a staircase ramp with varied success. The cheapest and easiest way to manufacture the spheres is to order them from a company working in metallurgy.

Starting from scratch, the overall cost is high (approximately 20,000 euros). The design and concept are a significant part of the cost of the project. This is why the experimental designs we have conceived are freely available on request for cultural uses and teaching, provided the CNRS and the designer of this experiment (J. Lilensten) are rightfully accredited.

Acknowledgements. We thank CNRS-SERAS group for their assistance in the engineering and design, O. Brissaud for his assistance in the assembly of the experiment, and Dr. J. Mc Auliffe (ESA/STEC) for his precious comments and careful reading of the present manuscript.

For commercial applications, the CNRS Alps delegation is the only partner entitled to negotiate the terms of collaboration.

References

Balescu, R. (1988), *Transport Processes in Plasmas*. Vol. 1, North-Holland, Amsterdam.

Bertaux, J.-L., F. Leblanc, O. Witasse, E. Quemerais, J. Lilensten, S.A. Stern, B. Sandel, and O. Korablev (2005), Discovery of an aurora on Mars, *Nature* **435**, 790-794, DOI: 10.1038/nature03603.

Chen, F.F. (1984), *Introduction to Plasma Physics and Controlled Fusion*, 2nd ed., Plenum Press, New York – London.

Dendy, R.O. (1995), *Plasma Physics. An Introductory Course*, Cambridge University Press, Cambridge.

Dortous de Mairan, J.J. (1733), *Traité Physique et Historique de l'Aurore Boréale*, De l'Imprimerie Royale, Paris, 281 pp.

Egeland, A., and W.J. Burke (2005), *Kristian Birkeland, the First Space Scientist*, Springer, New York, DOI: 10.1007/1-4020-3294-3.

Kivelson, M.G., and C.T. Russell (eds.), (1995), *Introduction to Space Physics*, Cambridge University Press, New York, 568 pp.

Kivelson, M.G., K.K. Khurana, C.T. Russell, R.J. Walker, J. Warnecke, F.V. Coroniti, C. Polanskey, D.J. Southwood, and G. Schubert (1996), Discovery of Ganymede's magnetic field by the Galileo spacecraft, *Nature* **384**, 6609, 537-541, DOI: 10.1038/384537a0.

Lilensten, J., and J. Bornarel (2006), *Space Weather, Environment and Societies*, Springer, Dordrecht, 242 pp, DOI: 10.1007/1-4020-4332-5.

Lummerzheim, D., and J. Lilensten (1994), Electron transport and energy degradation in the ionosphere: evaluation of the numerical solution, comparison with laboratory experiments and auroral observations, *Ann. Geophys.* **12**, 1039-1051, DOI: 10.1007/s00585-994-1039-7.

Rees, M.H. (1989), *Physics and Chemistry of the Upper Atmosphere*, Cambridge University Press, Cambridge – New York.

Shu, F.H. (1992), *The Physics of Astrophysics.* Vol. 2: Gas Dynamics, University Science Books, Sausalito, CA, 476 pp.

Stern, D.P. (1996), A brief history of magnetospheric physics during the space age, *Rev. Geophys*. **34**, 1, 1-32, DOI: 10.1029/95RG03508.

Received 25 April 2008
Accepted 13 November 2008